Nuclear Mass Formulas and its application for Astrophysics

Hiroyuki Koura

The Institute of Physical and Chemical Research (RIKEN),

Hirosawa 2-1, Wako, Saitama 1351-0198, JAPAN

Advanced Research Institute for Science and Engineering, Waseda University,

Okubo 3-4-1 , Shinjuku-ku, Tokyo 169-8555, JAPAN

koura@postman.riken.go.jp

koura@aoni.waseda.jp

Some nuclear mass formulas are reviewed and applied for the calculation of the rapid neutron-capture-process (r-process) nucleosynthesis. A new mass formula composed of the gross term, the even-odd term, and the shell term is also presented. The new mass formula is a revised version of the spherical basis mass formula published in 2000, that is, the even-odd term is treated more carefully, and a considerable improvement is brought about. The root-mean-square deviation of the new formula from experimental masses is 641 keV for $Z \geq 8$ and $N \geq 8$. Properties on systematic of the neutron-separation energy is compared with some mass formulas. The calculated abundances of the r-process from different mass formulas are compared with use of a simple reaction model, and the relation between the calculated abundances and the corresponding masses are discussed. Furthermore, fission barriers for the superheavy and neutron-rich nuclei are also applied for the endpoint of the r-process.

1 Introduction

Nuclear masses are important quantities to determine the ground-state properties and reactions. Since the Weizsäcker-Bethe nuclear mass formula [1, 2], many mass predictions were presented. At the present time, the main purpose of the study on mass formulas is not only to give more precise mass values of known nuclides but also to predict reliable masses of unknown nuclides, especially the superheavy nuclides and neutron-rich nuclides. As related to the latter, the mass predictions are required in the study of the abundance of the rapid-neutron-capture-process (r-process) nucleosynthesis because there are few experimental masses of neutron-rich nuclei related to the r-process.

In this report, we briefly review some mass formulas and outline our mass formula. The calculated r-process abundances with a simple reaction model from different mass formulas are compared. In our method of obtaining shell energies, fission barriers for the heavy and superheavy nuclei can be estimated. The application of these fission barriers for the r-process is also discussed.

2 Mass formula

One of the way to reproduce the known nuclear mass values is to use the mass systematics. For examples, the mass formulas by Comay et al. and Jänecke et al. [4] are based on the Garvey-Kelson-like systematics [3], and the root-mean-square (RMS) deviations from then current experimental masses are 350-450 keV. There is also the mass formula by Tachibana et al. [5] (TUYY formula) composed of a gross term with the Coulomb energy treated elaborately, an even-odd term, and an empirical shell term. The RMS deviation of it is about 550 keV. These phenomenological mass formulas are usable to reproduce known masses and unknown ones in the vicinity of known nuclei, however, these cannot be extrapolated to the region of superheavy nuclei where no empirical data are available: the above-mentioned mass formulas can be applied only for $N \leq$ 157-160. These formulas may also be difficult to predict the possibility of increasing or decreasing the strength of magicity far from the β-stability line. Moreover, no predictions of the nuclear shapes are available.

On the other hand, some approaches considering the nuclear force and the nuclear deformation have been done based on the models, or kinds of assumptions. The mass formula by Myers et al. [6] is the

early study of the liquid-drop model, which is composed of the macroscopic liquid-drop part and the microscopic shell part. (This early version were still in the similar problem to the above-mentioned systematics without the nuclear shapes). As examples of assumptions, we mention only two methods: the Skyrme-Hartree-Fock calculation and the relativistic mean-field calculation.

In the last decade, some mass predictions designed for the wide nuclidic regions were presented. We mention three mass predictions. One is the Finite-range droplet model (FRDM, 1995) formula, which is composed of the macroscopic droplet term and microscopic shell term [7]. The shell term is calculated from the folded-Yukawa single-particle potential. Other is the Hartree-Fock plus the BCS-type pairing method with the MSk7 Skyrme force (HFBCS-1, 2001) [8]. The last one is the mass formula by our groups published in 2000 [9], namely KUTY00. This formula is composed of the gross term, the even-odd term, and the shell term, and the first two terms are almost the same as those of TUYY formula. The method of obtaining the shell term is based on the spherical basis, and we solve some problems on the TUYY formula. These three methods can predict the nuclear shapes. The RMS deviations of these three predicted masses are about 600-800 keV in a current status. The differences of properties of these formulas will be discussed in the next section.

We now construct a new mass formula as a revised version of the KUTY00, that is, the even-odd term is treated more carefully, and a considerable improvement is brought about [11]. In the following, we give a brief explanation of the method of obtaining the shell energy and of the improved even-odd term.

Spherical basis mass formula with an improved even-odd term

Shell energy on a spherical basis

We first calculate shell energies for neutron groups and for proton groups in spherical nuclei using a spherical single-particle potential [10]. The potential parameters are assumed to be smooth functions of Z and N with the consideration of the charge symmetry, and this potential reproduces fairly well the single-particle levels of double-magic or magic-submagic nuclei in a wide nuclidic region. With this spherical potential, spherical shell energies can be obtained. For a spherical nucleus the nuclear shell energy is simply the sum of the refined spherical neutron and proton shell energies. The shell energy of a deformed nucleus is expressed as the sum of the intrinsic shell energy and the average deformation energy. The key point of the method to obtain the intrinsic shell energy is to treat the deformed nucleus as a particular superposition of spherical nuclei [9].

Improved even-odd term

The even-odd term of the new and the previous ones is expressed as

$$M_{\mathrm{eo}}(Z,N) = M_{\mathrm{odd}N}(Z,N)\delta_{\mathrm{odd}N} + M_{\mathrm{odd}N}(Z,N)\delta_{\mathrm{odd}N} - M_{\mathrm{oo}}(Z,N)\delta_{\mathrm{odd}N}\delta_{\mathrm{odd}Z} \tag{1}$$

with

$$\delta_{\mathrm{odd}i} = \begin{cases} 0 & \text{for even-}i \\ 1 & \text{for odd-}i,\ i=N \text{ and } Z. \end{cases} \tag{2}$$

In the previous mass formula [5, 9], the construction of the even-odd term was insufficient mainly in two points. One is the functional form of $M_{\mathrm{odd}Z}(Z,N)$ and $M_{\mathrm{odd}N}(Z,N)$. Considering the charge symmetry of the nuclear force, we also take the functional form of the charge symmetry for odd-N and odd-Z terms as treated generally. The charge symmetry requires that the magnitudes of $M_{\mathrm{odd}Z}(Z,N)$ and $M_{\mathrm{odd}N}(Z,N)$ between mirror nuclei are equal to each other. When we have compared the "experimental" $M_{\mathrm{odd}Z}^{\mathrm{exp}}(Z,N)$ and $M_{\mathrm{odd}N}^{\mathrm{exp}}(Z,N)$ between mirror nuclei, however, the result is different. There are 45 pairs of mirror nuclei in the experimental data and almost all of $M_{\mathrm{odd}N}^{\mathrm{exp}}(a,b) - M_{\mathrm{odd}Z}^{\mathrm{exp}}(b,a)$ (a: even, b: odd) is positive, and the average is about 100 keV. This means that the even-odd term for a proton is somewhat smaller than that for a neutron. Undoubtedly, the main reason for this is the Coulomb repulsive force between protons. (More precise discussion, see Ref. [11]). Considering the above features of "experimental" even-odd term, we make the functional form of the even-odd term. The other point is the odd-odd term $M_{\mathrm{oo}}(Z,N)$. In the previous formula, $M_{\mathrm{oo}}(Z,N)$ is a function independent on

$M_{\mathrm{odd}Z}(Z, N)$ and $M_{\mathrm{odd}N}(Z, N)$. $M_{\mathrm{oo}}(Z, N)$ is caused by the interaction between the last odd-neutron and the last odd-proton. This interaction seems to be weaker than the pairing interaction, and $M_{\mathrm{oo}}(Z, N)$ should be smaller than either of $M_{\mathrm{odd}Z}(Z, N)$ and $M_{\mathrm{odd}N}(Z, N)$. In the new formula, we impose this constraint on the form of $M_{\mathrm{oo}}(Z, N)$.

3 Properties of recent mass formulas

The root-mean-square (RMS) deviation is given in Table 1. The RMS deviation of our present formula, we refer to as KTUY02, is 657.7 keV for 1835 experimental masses [12], which is smaller than that of the KUYT00 mass formula [9], 680.2 keV. In Table 1, we also list the RMS deviations of two other recent mass formulas, FRDM [7] and HFBCS-1 [8]. Among them, our mass formula has the smallest RMS deviation. Although there is not much difference in the RMS deviations among these three mass formulas, there still remain fairly large differences of the estimated masses for some individual nuclides. The RMS deviation of the separation energies of KTUY02 mass formula is listed in Table 2 together with those of the two others. Our RMS deviation is significantly smaller than those of the others.

Figure 1 shows the two-neutron separation energies $S_{2\mathrm{n}}$ for even-N, the experimental data in (a), our results in (b), ones of FRDM in (c), and HFBCS in (d). We connect the nuclei with the same N by solid lines. In such a figure, magicities are seen as large gaps between two lines. In the panel (a), we see large gaps between $N=8$ and 10 (abbreviated as "at $N=8$"), and at $N=20$, 28, 50, 82, 126 except for the region with very small values of $S_{2\mathrm{n}}$. Similar gaps are seen in the other panels without ones at $N=8$ and $N=20$. On the very neuron-rich region, which corresponds to the region near the $S_{2\mathrm{n}}=0$ line, the large gaps of $S_{2\mathrm{n}}$ for (b) at $N=20$, 28, 50 decrease , and the gaps at $N=16$, 32 (or 34), 58 become larger compared with the neighboring ones. On the other hand, in the panel (c) the decreasing the magic gaps are not so clear, and unreasonable crossing of the solid lines are shown in the region of the very neutron-rich nuclei. In the panel (d), the similar tendencies on increasing the gaps seem to be seen at $N=16$ and 34, but the gap at $N=20$ and 28 is not so clear compared with those of experimental data and ours, and some unreasonable zigzag lines are seen in the region of heavy and neutron-rich nuclei.

4 Application for astrophysics

4.1 R-process abundances

It is considered that about half of the stable nuclides heavier than iron observed in nature are synthesized by the rapid neutron-capture process (r-process). We estimate the nuclidic abundances produced in the r-process nucleosynthesis in the canonical model with the waiting point approximation [13]. For each N, the most abundant isotope has an even neutron number N, and its two-neutron separation energies $S_{2\mathrm{n}}(Z, N)$ satisfies the constraints [14]

$$S_{2\mathrm{n}}(Z, N+2)/2 \leq S_a^0 \equiv (34.075 - \log N_{\mathrm{n}} + 1.5 \log T_9) \times T_9/5.04 \leq S_{2\mathrm{n}}(Z, N)/2, \tag{3}$$

where N_{n} is the neutron number density in cm^{-3} and T_9 is the temperature in 10^9 K. The r-process path in the N-Z plane is defined as the ensemble of the nuclides satisfying the above equation. The equation of the time evolution is written as

$$\frac{dY_Z(t)}{dt} = -\lambda_Z Y_Z(t) + \lambda_{Z-1} Y_{Z-1}(t), \tag{4}$$

where Y_Z is the sum of abundance $Y(Z, N)$ and λ_Z is the sum of the decay constant λ with the same Z.

We take the $S_{2\mathrm{n}}$ from some mass formulas, and the values of λ are estimated from theoretical β-decay half-lives [16] with Q_β of mass formulas, and N_{n}, T_9, τ are chosen so as to reproduce the abundance peak at $A = 130$. Figure 2 shows the r-process abundances for three mass formulas. Focused on the abundance around $A = 130$, the lack of the abundances is seen at $A \approx 110$ for those of KUTY, and the deeper dips are seen for those of FRDM. These results could be explained with the tendencies of the neutron-separation energies. Figure 3 shows two-neutron separation energies $S_{2\mathrm{n}}$ connected with isotopes. In the panels of TUYY and KUTY, the isotope lines of $S_{2\mathrm{n}}$ go regularly, In the right panel of FRDM, however, the lines of $Z=36$-40 and some neighboring ones have the dips around $N=40$-44 and $N=70$-80. Because experimental

S_{2n} of the nuclei around Z=38 and N=40 exist and no corresponding dips are seen, the dips of FRDM around N=40-44 seem to be incorrect. On the other hand, there are no experimental data corresponding nuclei with the dips of FRDM around N=70-80, but the both TUYY and KUTY formulas have no corresponding dips. The dips around N=70-80 correspond to $A \approx$110 on the r-process abundances. If the isotope lines have the dips and these values satisfy the condition of Eq. (3), the calculated abundances diffuse into the nuclei with the different N, and consequently there are fewer abundances compared with the neighboring ones. The dips around N=70-80 of FRDM also cause the lack of the abundances at $A \approx$110. It is noted that the predicted nuclear shapes by FRDM change from the prolate shapes to the oblate ones in the two regions. As for the lack of abundances around $A \approx 110$ of KUTY, the isotope lines with Z=36-40 of KUTY have gentler slopes in the corresponding region compared with those of TUYY. The difference of steepness causes less abundances of KUTY than those of TUYY, although more than those of FRDM. Figure 2 also shows the decreasing of the abundances in the region of $A > 150$ for KUTY and FRDM. These differences are caused by the different mass surfaces. These results are not so critical, at present, because we take a simple reaction model in which such a bulk feature cannot be considered. If we take more realistic reaction model, the situation seems to change, but the problem related to the dips on the above-mentioned S_{2n} systematics is still remaining.

4.2 Fission-barrier height relevant to r-process

After the end of the rapid neutron capture, the synthesized nuclei go to the beta-stable region by the beta-decay. However, if the fission barrier B_{fiss} of a daughter nucleus is lower than the beta-decay Q-value Q_β of a parent nucleus, such a nucleus is not expected to reach the beta-stable nuclei because of the fission. Now, we estimate the beta-decay Q-values from the present mass formula, KTUY02, and the fission-barrier heights with use of the method of obtaining the spherical basis shell term [15]. Figure 4 shows the region with $Q_\beta - B_{fiss} > 0$. The r-process paths obtained the previous subsection are also seen. This figure shows the existence of the nuclei with $Q_\beta - B_{fiss} > 0$ in the region with nuclei around $Z \approx$106 and $N \approx$192. These nuclei are located between the r-process path and the β-stability line. This indicates that superheavy nucleus $^{298}[114]_{184}$ is not expected to be synthesized from the r-process.

Acknowledgement

References

[1] C.F. von Weizsäcker, Z. Phys. **96** (1935) 431.

[2] H.A. Bethe and R.F. Bacher, Rev. Mod. Phys. **8** (1936) 829.

[3] G.T. Garvey, *et al.*, Rev. Mod. Phys. **41**, (1969) S1.

[4] P.E. Haustein, Special Editor: "*1988-89 Atomic Mass Predictions*", ATOMIC DATA AND NUCLEAR DATA TABLES **39** (1988) 185.

[5] T. Tachibana, M. Uno, M. Yamada, S. Yamada, ATOMIC DATA AND NUCLEAR DATA TABLES **39** (1988) 251.

[6] W.D. Myers, W.J. Swiatecki, Nucl. Phys. **81** (1966) 1.

[7] P. Möller, J.R. Nix, W.D. Myers, J. Swiatecki, ATOMIC DATA AND NUCLEAR DATA TABLES **59**, (1995) 185.

[8] S. Goriely, F. Tondeur, J.M. Pearson, ATOMIC DATA AND NUCLEAR DATA TABLES **77** (2001) 311.

[9] H. Koura, M. Uno, T. Tachibana, M. Yamada, Nucl. Phys. **A674** (2000) 47; H. Koura, M. Uno, T. Tachibana, M. Yamada, RIKEN-AF-NP-394, RIKEN (2001).

[10] H. Koura and M. Yamada, Nucl. Phys. **A 671** (2000) 96.

[11] H. Koura, T. Tachibana, M. Uno, M. Yamada, in preparation.

[12] G. Audi and A.H. Wapstra, Nucl. Phys. **A 595** (1995) 409.

[13] T. Kodama, K. Takahashi, Nucl. Phys. **A239** (1975) 489.

[14] T. Tachibana, M. Arnould, Nucl. Phys. **A588** (1995) 333c.

[15] H. Koura, J. Nucl. Radiochem. Sci. **3** (2002) 201.

[16] T. Tachibana, M. Yamada, T. Yoshida, Prog. Theor. Phys. **84** (1990) 641.

Table 1: RMS deviations of mass formulas from experimental data in keV. The values in the parentheses are the numbers of nuclei.

Mass formula	nuclidic region	
	$Z, N \geq 2$ (1835)	$Z, N \geq 8$ (1768)
KTUY02 (this work)	657.7	640.8
KUTY00	680.2	656.1
FRDM	-	678.3
HFBCS-1	-	718.0

Table 2: RMS deviations of separation energies from experimental data for their mass formulas in keV. The values in the parentheses are the numbers of nuclei.

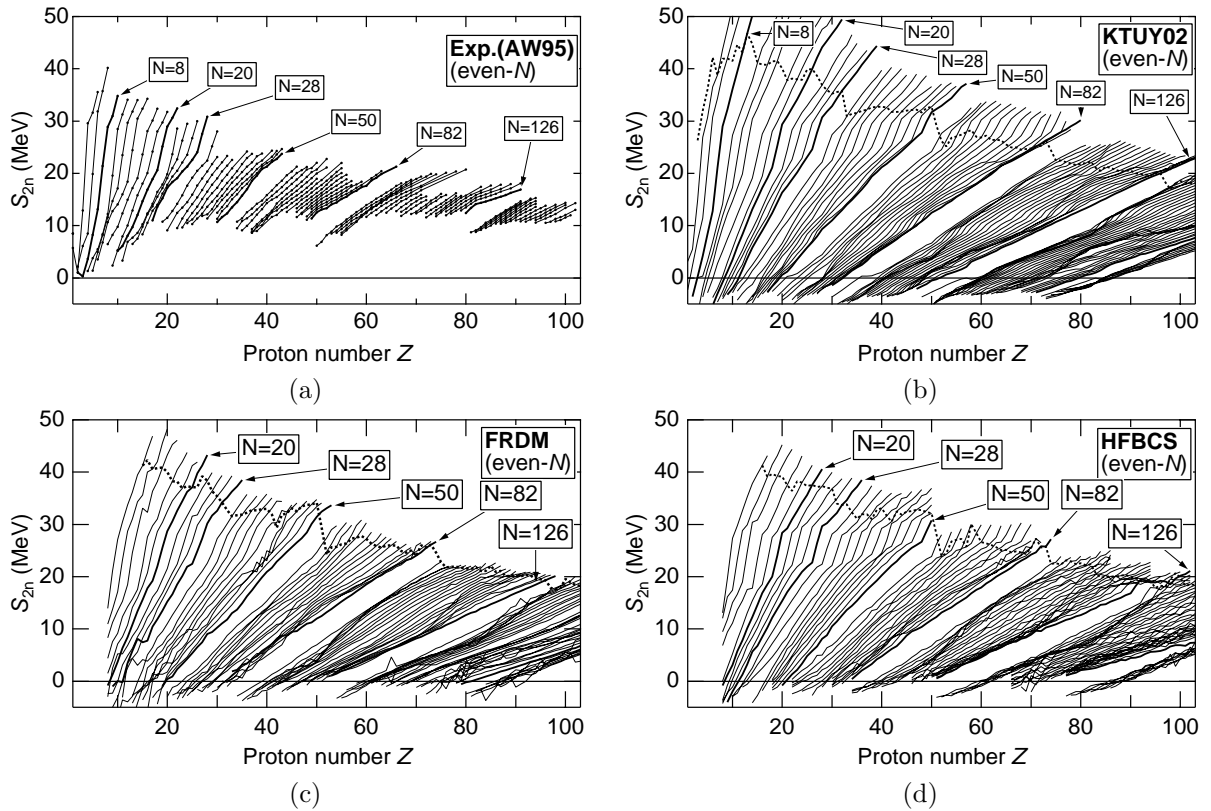| Mass formula	neutron		proton	
	S_{n}	S_{2n}	S_{p}	S_{2p}
$Z, N \geq 2$	(1648)	(1572)	(1592)	(1483)
KTUY02	361.7	466.0	403.1	542.0
$Z, N \geq 8$	(1585)	(1515)	(1527)	(1424)
KTUY02	319.1	391.9	344.4	465.8
FRDM	416.7	551.6	409.0	514.2
HFBCS-1	464.6	506.1	483.3	529.0

Figure 1: Two-neutron separation energies S_{2n} for even-N. The solid lines connect the nuclei with the same N, and dashed line comments the proton-drip nuclei for fixed N's. (a): experimental data, (b): KTUY02 (present formula), (c): FRDM, (d): HFBCS.
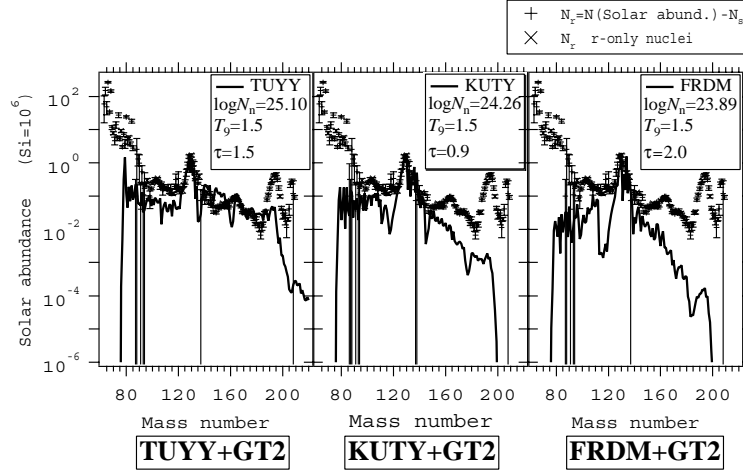
Figure 2: Relative r-process abundances estimated by using the canonical model. The crosses represent the solar system r-process abundances. Observed and calculated abundances are normalized to ^{130}Te.
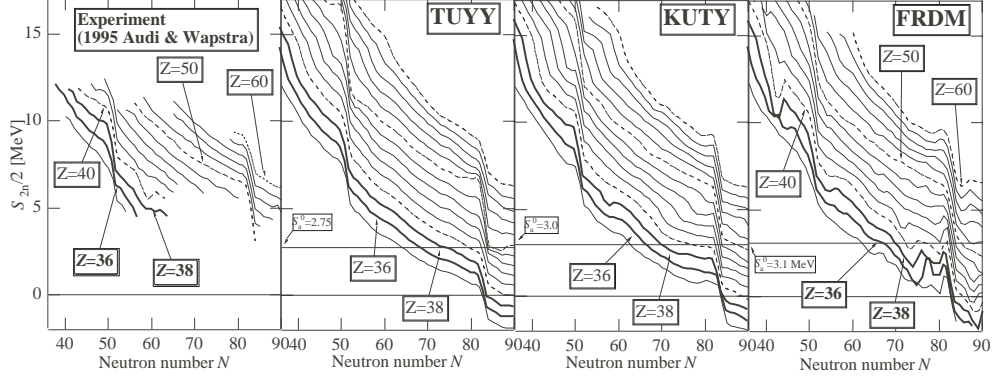

Figure 3: Two-neutron separation energies S_{2n} for even-Z. The solid lines connect the nuclei with the same Z. The S_a^0 line defined in Eq. (3) for each mass formula is also shown.
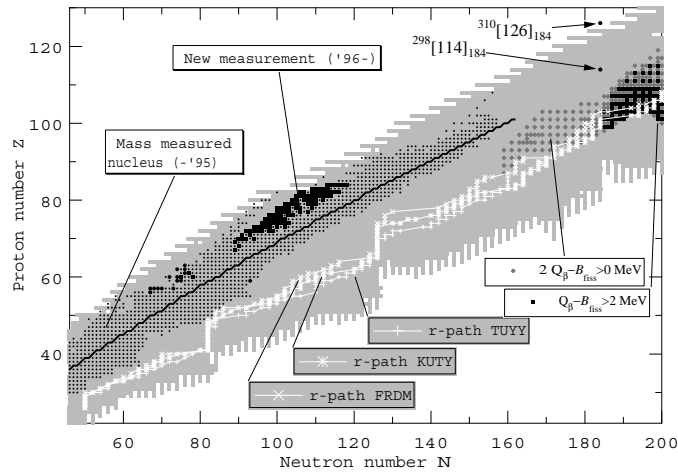

Figure 4: The r-process paths for each mass formula and the nuclei with $Q_\beta - B_{\text{fiss}} > 0$ estimated from the KUTY mass formula.